Germanium-on-silicon nitride waveguides for mid-infrared integrated photonics

Li, Wei; Anantha, P.; Bao, Shuyu; Lee, Kwang Hong; Guo, Xin; Hu, Ting; Zhang, Lin; Wang, Hong; Soref, Richard; Tan, Chuan Seng

2016

Li, W., Anantha, P., Bao, S., Lee, K. H., Guo, X., Hu, T., et al. (2016). Germanium-on-silicon nitride waveguides for mid-infrared integrated photonics. Applied Physics Letters, 109(24), 241101-.

https://hdl.handle.net/10356/83584

https://doi.org/10.1063/1.4972183

Germanium-on-silicon nitride waveguides for mid-infrared integrated photonics

Wei Li,[1] P. Anantha,[1] Shuyu Bao,[1,2] Kwang Hong Lee,[2] Xin Guo,[1] Ting Hu,[1] Lin Zhang,[1] Hong Wang,[1] Richard Soref,[3] and Chuan Seng Tan[1,2,a)]

[1]*School of Electrical and Electronic Engineering, Nanyang Technological University, 50 Nanyang Avenue, Singapore 639798*

[2]*Low Energy Electronic System (LEES), Singapore-MIT Alliance for Research and Technology (SMART), 1 CREATE Way, #09-01/02 CREATE Tower, Singapore 138602*

[3]*Engineering Department, University of Massachusetts at Boston, 100 Morrissey Blvd., Boston, Massachusetts 02125, USA*

(Received 6 September 2016; accepted 1 December 2016; published online 14 December 2016)

A germanium-based platform with a large core-clad index contrast, germanium-on-silicon nitride waveguide, is demonstrated at mid-infrared wavelength. Simulations are performed to verify the feasibility of this structure. This structure is realized by first bonding a silicon-nitride-deposited germanium-on-silicon donor wafer onto a silicon substrate wafer, followed by the layer transfer approach to obtain germanium-on-silicon nitride structure, which is scalable to all wafer sizes. The misfit dislocations which initially form along the interface between germanium/silicon can be removed by chemical mechanical polishing after layer transfer process resulting in a high-quality germanium layer. At the mid-infrared wavelength of 3.8 μm, the germanium-on-silicon nitride waveguide has a propagation loss of 3.35 ± 0.5 dB/cm and a bend loss of 0.14 ± 0.01 dB/bend for a radius of 5 μm for the transverse-electric mode. *Published by AIP Publishing.*
[http://dx.doi.org/10.1063/1.4972183]

Silicon-based photonics has drawn much attention in recent years due to its compatibility with the CMOS process as well as its possibility of integration with microelectronics.[1] Researchers have been trying to extend the operation wavelength of photonics to mid-infrared (MIR) defined here as 2–15 μm because of the promising applications in MIR such as next generation communication, biochemical sensing, environment monitoring and so on.[2,3] The standard silicon-on-insulator (SOI) is not suitable for MIR since the material loss of the buried oxide layer becomes substantially high at 3.7 μm and beyond. Many efforts have been put to look for an alternative material system that can work in MIR. The silicon-on-sapphire (SOS) waveguide technology has been pursued to extend the operation wavelength range up to 4.4 μm.[4] Silicon-on-nitride (SON) waveguides, providing a wide transparent range of 1.2–6.7 μm, also have been proposed.[5] Germanium (Ge) has a wide transparency and many optical properties[6–8] making it a good alternative for SOI, thus many Ge-based platforms have been proposed and studied. Germanium-on-insulator (GOI) has been proposed and passive waveguides and active Ge modulator have been fabricated on the platform but the buried oxide layer actually limits the transparency of this platform as mentioned above.[9] Germanium-on-SOI has also been reported with its electrical advantages.[10] Germanium-on-silicon (GOS) platform is widely used in photonics research presently and many impressive achievements have been done.[11–13] The lowest propagation loss Ge waveguides on that platform reported only to have had a loss of 0.6 dB/cm.[14] However, the refractive index contrast between Ge ($n = 4.1$)[15] and Si ($n = 3.4$)[15] is considerably less than that of SOI ($\Delta n = 2.01$). The numbers of refractive indices are at 3.8 μm. As a result, the bend radii in GOS must be accordingly larger than those in SOI, causing the footprint of GOS on-chip devices to be generally larger than those of SOI. What is desired is a better alternative Ge-waveguide platform that will provide a larger core-clad index contrast than GOS as well as useful transparency and smaller channel-bend radii. To achieve these goals, the structure proposed and realized in this work is *Germanium-on-Silicon Nitride* referred to here as GON. The refractive index of our PECVD silicon nitride (SiN_x) is measured by an ellipsometer, and it is 1.9 at 3.8 μm. SiN_x is typically transparent up to about 7.5 μm. So the index contrast in GON is 2.2. Upon realizing this Ge platform operating in the MIR range, there would be many passive photonic devices that can be fabricated with a compact footprint such as Mach-Zehnder interferometers, micro-ring resonators, and so on. To make a compact ring, a small bend radius is required, and this in turn is only possible with high-contrast waveguides having strong optical confinement.[16] Moving forward, compact sensing devices[17] can also be realized based on micro-ring resonators[18] with this Ge platform. Most importantly, we have developed a feasible and scalable wafer bonding and layer transfer technique to realize GON.

Firstly, modeling has been performed to study the feasibility of bent waveguides with smaller radius realized on the GON platform. Finite difference time domain method (FDTD) was utilized to verify the lower waveguide-bend propagation loss of GON versus GOS. Assuming an operation wavelength of 3.8 μm, the thickness of the Ge strip core and the SiN_x layer thickness were set to be 1 μm each. The cross sectional dimensions of both waveguides on these two platforms were determined to support a single TE mode propagation and the mode profiles are illustrated in Figure 1.

a)Electronic mail: tancs@ntu.edu.sg

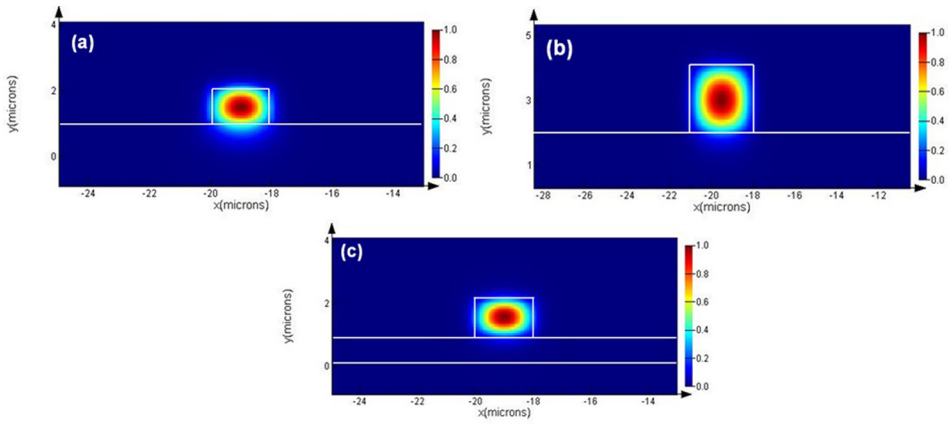

FIG. 1. Simulation results (a) mode profile of waveguide on GOS with width = 2 μm and height = 1 μm; (b) mode profile of waveguide on GOS with width = 3 μm and height = 2 μm; (c) mode profile of waveguide on GON with width = 2 μm and height = 1 μm.

The simulation results demonstrate that only single modes are allowed at the size of core. From simulation results, it can be observed that GON has a better confinement on the mode at the core-cladding interface which is 4% less compared to the mode of GOS at the interface according to the overlap analysis. Unit power was launched into a 90° bend whose inner radius R was varied from 2 to 18 μm. Figure 2 shows the bend loss of the waveguide as a function of R and the cross sectional dimension of waveguide on GOS was also changed to demonstrate that the GON has a better confinement on the propagating mode even with a smaller dimension. WG in Figure 2 stands for "waveguide" and different cross-sectional dimensions are indicated in the annotation of Fig. 2. This simulation reveals the smaller bend loss of waveguides on GON. Specifically, at $R = 5$ μm, GON has a loss of ~0.013 dB/bend versus ~1.74 dB/bend of WG4 on GOS. The performance gap becomes wider as the bend radius decreases. Therefore this GON structure has the potential for compact efficient networks on-chip. The bend loss of the bent waveguides on GOS shows gradual improvement as the cross-sectional dimensions increase showing that mode confinement is better in GON, allowing smaller $W \times H$.

The Ge/Si platform can be fabricated by several techniques. These include Ge condensation,[19] liquid phase epitaxy,[20] and layer transfer techniques.[21] However, when Ge is grown directly on SiN_x, the quality of the Ge crystal is expected to be poor and a high density of defects is formed at the interface since SiN_x is amorphous. As a result, these defects will increase the scattering loss. In this work we utilize the *wafer bonding and layer transfer* technique to fabricate the GON as summarized in Fig. 3. In this process, 1.5 μm thick single crystal Ge is grown on a 6-in. Si donor wafer using reduced pressure chemical vapor deposition (RPCVD) with three-step Ge growth method.[22] The Ge epilayer is then coated with silicon nitride and transferred to another Si substrate to obtain the GON wafer. For comparison, some Ge-on-Si (GOS) wafers (grown in similar manner but not transferred) are included in the subsequent experiments. The final Ge layer has a threading dislocation density (TDD) typically $<5 \times 10^6\,cm^{-2}$, surface roughness <1 nm, and a tensile strain of 0.2%.[23] Further, cleaning of the donor wafer is carried out to obtain a surface free of oxide and contaminants, followed by a deionized water (DI water) rinsing and N_2 drying. After the cleaning process, the donor wafer is loaded into a Cello PECVD system for the deposition of tensile strained SiN_x. A post deposition annealing for several hours can ensure the release of gases trapped in the wafer during the deposition process. All the thermal processes are done at a temperature below 400 °C. Further, another 1 μm of SiN_x is deposited on the backside of the wafer to compensate for the bowing effect. The final deposition of 300 nm of the bonding layer is processed via low temperature PECVD. This bonding layer is SiO_2 which enables the ease of bonding with another Si handle wafer. Since a hydrophilic type of bonding is used in this work, there will be water molecules forming during the bonding reaction. Therefore, SiO_2 is chosen as the bonding layer as it can absorb these water molecules hence providing a high bonding quality.[24] The bonding layer is subjected to chemical mechanical polishing (CMP) down to 100 nm, in order to reduce the surface roughness so that it is suitable for wafer bonding. The donor wafer can then be bonded onto a Si substrate wafer. Prior to bonding, both the wafer surfaces are to be exposed to O_2 plasma for about 15 s to improve the hydrophilicity of the surface. After that, a DI water rinsing step is incorporated to improve the density of the surface hydroxyl group to initiate bonding. The bonded wafer pair is then subjected to post-bond annealing at a temperature below 300 °C for about 4 h to improve the bond strength. The bonded wafer is inspected using IR imaging to check for the formation of interfacial voids. To complete the layer transfer process, the top Si donor wafer is subjected to grinding in order to transfer the Ge/SiN_x layer

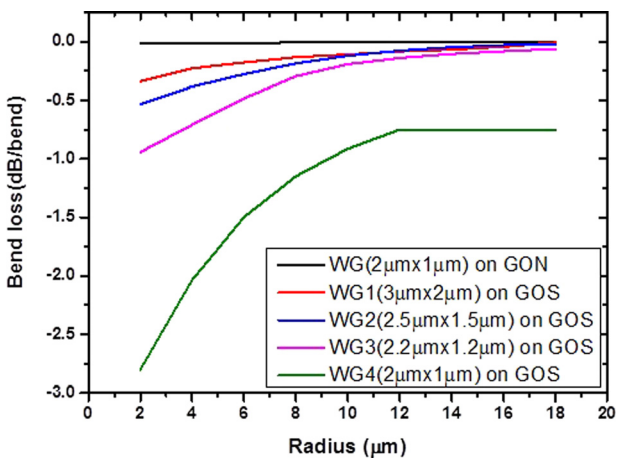

FIG. 2. Simulated bend losses in GON compared to those in GOS, showing lower bend losses of waveguides on GON.

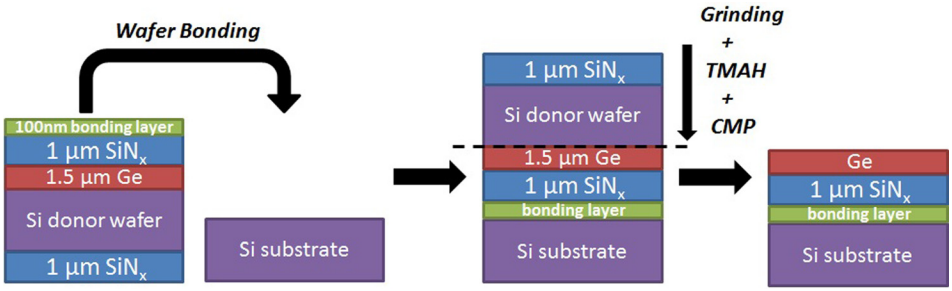

FIG. 3. Wafer bonding and Layer transfer process to obtain Ge on SiN_x structure is illustrated. The bonding layer refers to SiO_2.

stack on the substrate wafer. This is followed by wet etching using tetramethylammonium hydroxide (TMAH) to completely remove the Si donor wafer. Given the high selectivity of TMAH for Si over Ge, etch stop takes place at the original Ge/Si interface. This Ge/Si interface layer will then be removed by chemical and mechanical polishing (CMP). Our process uses two silicon wafers, the Si donor and the Si substrate wafers, and is therefore scalable to all wafer sizes. X-ray Diffraction (XRD) analysis was used to characterize the Ge film quality with reference to the GOS after the fabrication of GON wafer and the results are shown in Figure 4. The XRD analysis shows that the crystal quality of Ge epilayer on GON does not change significantly as signified by the peak intensity and curve shape that are comparable with that of the Ge on Si wafer. The Ge peaks are shifted to the right with reference to the Ge bulk substrate as a result of a tensile strain (due to thermo-mechanical mismatch) which is 0.17% for GOS and 0.13% for GON, respectively. The 0.04% strain relaxation is due to the removal of Si donor wafer and this tensile strain will not affect the transparency of Ge at 3.8 μm.

We have fabricated waveguides on GON and GOS wafers to verify our simulation results. In the simulation, we set the width and height of the waveguide to be 2 μm and 1 μm, respectively, thus the GON wafer is thinned down by CMP to obtain 1 μm thick Ge. Post CMP, the Ge layer is patterned using standard optical lithography. Reactive Ion Etching (RIE) in Oxford Plasmalab 80 with Cl_2 gas is utilized to etch the Ge layer all the way down to SiN_x layer to form the strip waveguide. The final Ge strip waveguide has a width of $\sim$2 μm and a height of $\sim$1 μm (Fig. 5(a)). SEM

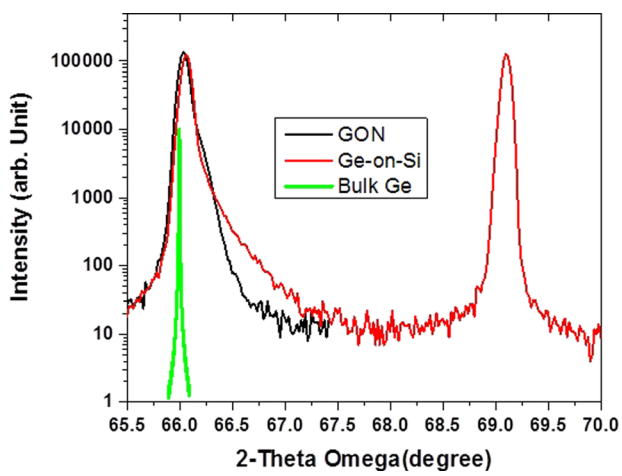

FIG. 4. The XRD profile of the Ge epilayers on GON and GOS with reference to bulk Ge.

images at different orientations have also been taken to show the sidewall quality (Fig. 5(b)). It can be seen from Fig. 5(a) that the sidewalls are not very vertical using RIE with a power of 200 W and chamber pressure of 20 mT. What's more, the quality of the surface of the sidewall which can be observed from Fig. 5(b) is not perfect.

The propagation loss and bend loss measurements are carried out by employing the cut-back method.[25] This method is based on a comparison of transmission through waveguides of different lengths or number of bends and fitting the dependence on the length or number of bends assuming identical coupling conditions and an identical surface roughness. We have fabricated waveguides whose total length changes from 2 mm to 12 mm with a step of 2 mm. Each waveguide has 8 bends ($R = 50$ μm) and we assume that the total bend loss in 8 bends at this large radius is negligible.

The device under test is mounted on a XYZ translational stage. Light source with 3.8 μm wavelength from a rapid-scan CW-Pulsed quantum cascade laser of DAYLIGHT SOLUTIONS goes through a polarization controller and is then coupled into a single mode ZrF_4 fiber from Thorlabs. In our measurements, we choose the TE mode for each measurement. Further, the fiber tip is aligned with the facet of the strip waveguide for coupling the light into the waveguide. For efficient and reproducible coupling from a fiber to single mode waveguides, taper geometry were designed on each side of the waveguides with a total length of 800 μm, long base of 20 μm, and short base of 2 μm. After passing through the device, the light is collected by a similar fiber as that at the input. The output power of the light is analyzed by an InSb photodiode photodetector with a high sensitivity from HORIBA. Same waveguides were also fabricated on GOS wafer using the same processes, in order to make a comparison. All the devices have been measured multiple times to ensure repeatability and the results are confirmed to be reproducible. The propagation loss measurement results are shown in Figure 6. It can be seen that the propagation loss of waveguide on GOS is 8.18 ± 0.6 dB/cm which is much higher than that of the waveguide on GON whose propagation loss is 3.35 ± 0.5 dB/cm. The higher propagation loss of GOS wafer is mainly caused by the poor confinement of the propagating mode. The mode has larger overlaps with the sidewall and the interface between Ge and Si. There are misfit dislocations in the interface because of the lattice mismatch between Ge and Si. However, the misfit dislocations which are previously hidden along the Ge/Si interface now can be exposed on the top of the wafer with layer transfer method and can be removed by CMP. The defective layer actually was removed when we performed CMP to thin

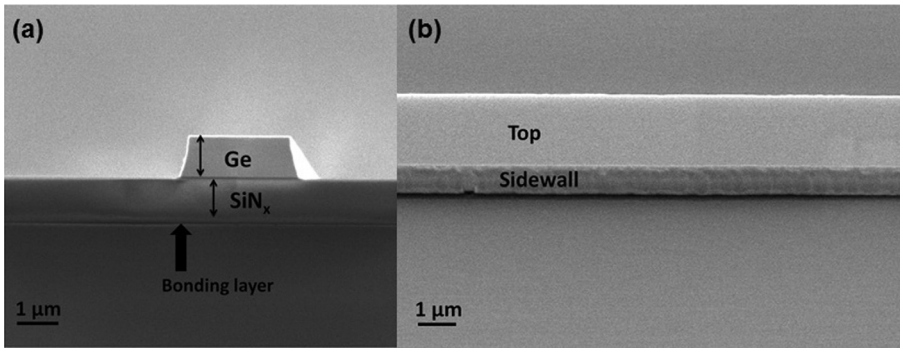

FIG. 5. (a) Cross-sectional image of patterned GON wafer; (b) SEM image at a different orientation to show the sidewall quality.

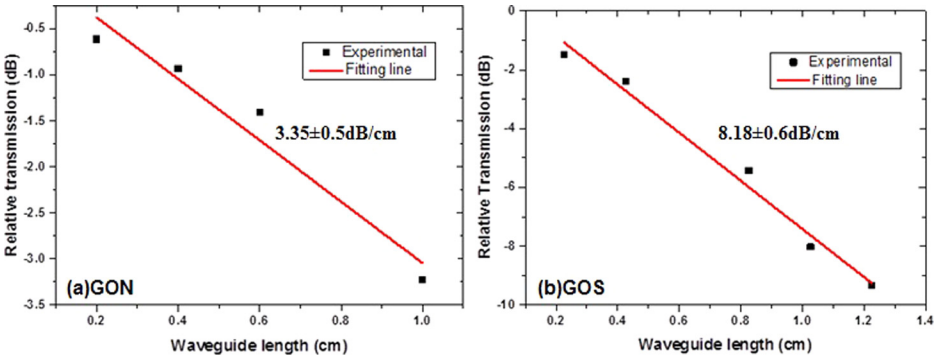

FIG. 6. Measurement results of propagation losses of waveguides on GON and GOS wafers. GON wafer has a propagation loss of 3.35 ± 0.5 dB/cm, while GOS has a propagation loss of 8.18 ± 0.6 dB/cm.

down the Ge layer to 1 μm after wafer bonding and layer transfer. The propagation loss of GON can be further reduced with a better quality of sidewall in the waveguides to reduce the scattering loss, which can be realized by better precision in lithography and deep silicon etching. For certain applications, we can design the rib structure to realize a better mode confinement thus further reducing the propagation loss.[14]

We have also fabricated the bent waveguides with a radius of 5 μm on GON and GOS for comparison. The number of 90° bends on both wafers varies from 4 to 36. The bend loss measurement results are illustrated in Figure 7. As shown in Fig. 7, the bend loss of waveguides on GON is much smaller than that on GOS due to the better confinement, and the bend loss is only 0.14 ± 0.01 dB/bend compared to 2.54 ± 0.15 dB/bend of that on GOS. The total length of each waveguide is fixed at 5 mm and the length of the straight waveguide decreases as the number of bends increase. The influence of the length change has been ruled out when we calculated the bend loss using the propagation loss of 3.35 dB/cm. The higher bend loss of GOS is because the mode interacted intensively with the interface and sidewall due to poor optical confinement. The largest source of bend loss is actually the mode mismatch loss. It is due to the imperfect mode overlap between the straight and the bent waveguides. This leads to scattering at the start and end of fixed-radius bends. We expect to further reduce the bend loss of GON by varying the curvature of the bend continuously rather than abruptly.[26] There is discrepancy between the simulation and measurement results of bend loss because the sidewall is assumed to be free of roughness in the simulation which means that there is no scattering loss caused by the interaction between light mode and waveguide sidewall. However, this loss cannot be ignored in real measurements.

In summary, a Ge based platform was proposed and fabricated. The defective layer containing misfit dislocation can be exposed by layer transfer and removed by CMP, thus providing a high-quality Ge layer on SiN_x under the cladding layer. Simulation was carried out to study the feasibility of GON platform for providing smaller channel-bend radii. Waveguides were fabricated on the GON wafer and were characterized at the 3.8 μm wavelength. The bend loss on GON at radius of 5 μm is 0.14 ± 0.01 dB/bend and the propagation loss is 3.35 ± 0.5 dB/cm. These losses are expected to be further reduced by improving the sidewall quality with advanced processes like E-beam lithography and Deep RIE

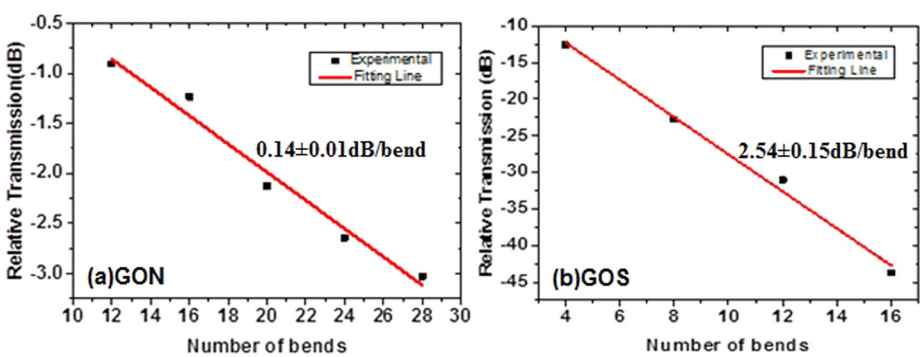

FIG. 7. Measurement results of bend losses on GON and GOS. The bend loss of GON is 0.14 ± 0.01 dB/bend and the bend loss of GOS is 2.54 ± 0.15 dB/bend.

or by a different structure. This GON platform has potential making passive photonic devices with small footprint possible which can be useful for compact sensor devices on-chip for MIR sensing applications, as well as for active devices like micro-ring modulators.

This work was supported by the National Research Foundation of Singapore (NRF-CRP12-2013-04). RS thanks the AFOSR for support.We thank the Silicon—Center of Excellence for the use of testing equipment.

[1]R. Soref, IEEE J. Sel. Top. Quantum Electron. **12**(6), 1678 (2006).
[2]B. E. A. Saleh, M. C. Teich, and B. E. Saleh, *Fundamentals of Photonics* (Wiley New York, 1991).
[3]R. Soref, Nat. Photonics **4**(8), 495 (2010).
[4]T. Baehr-Jones, A. Spott, R. Ilic, A. Spott, B. Penkov, W. Asher, and M. Hochberg, Opt. Express **18**(12), 12127 (2010).
[5]S. Khan, J. Chiles, J. Ma, and S. Fathpour, Appl. Phys. Lett. **102**(12), 121104 (2013).
[6]H. H. Li, J. Phys. Chem. Ref. Data **9**(3), 561 (1980).
[7]C. Wolff, R. Soref, C. G. Poulton, and B. J. Eggleton, Opt. Express **22**(25), 30735 (2014).
[8]C. Bubeck, V. Degiorgio, and C. Flytzanis, "Nonlinearities of Conjugated Polymers and Dye Systems," in *Nonlinear Optical Material: Principles and Applications*, edited by V. Degiorgio and C. Flytzanis (IOS Press, Amsterdam, 1995), p. 359.
[9]J. Kang, M. Takenaka, and S. Takagi, Opt. Express **24**(11), 11855 (2016).
[10]U. Younis, S. K. Vanga, A. E.-J. Lim, P. G.-Q. Lo, A. A. Bettiol, and K.-W. Ang, Opt. Express **24**(11), 11987 (2016).
[11]A. Malik, M. Muneeb, Y. Shimura, J. Van Campenhout, R. Loo, and G. Roelkens, Appl. Phys. Lett. **103**(16), 161119 (2013).
[12]L. Shen, N. Healy, C. J. Mitchell, J. S. Penades, M. Nedeljkovic, G. Z. Mashanovich, and A. C. Peacock, Opt. Lett. **40**(2), 268 (2015).
[13]N. J. D. Martinez, C. T. DeRose, R. W. Brock, A. L. Starbuck, A. T. Pomerene, A. L. Lentine, D. C. Trotter, and P. S. Davids, presented at the *IEEE Optical Interconnects Conference (OI)* (2016).
[14]M. Nedeljkovic, J. S. Penadés, C. J. Mitchell, A. Z. Khokhar, S. Stanković, T. D. Bucio, C. G. Littlejohns, F. Y. Gardes, and G. Z. Mashanovich, IEEE Photonics Technol. Lett. **27**(10), 1040 (2015).
[15]H. W. Icenogle, B. C. Platt, and W. L. Wolfe, Appl. Opt. **15**(10), 2348 (1976).
[16]W. Bogaerts, P. De Heyn, T. Van Vaerenbergh, K. De Vos, S. K. Selvaraja, T. Claes, P. Dumon, P. Bienstman, D. Van Thourhout, and R. Baets, Laser Photonics Rev. **6**(1), 47 (2012).
[17]A. Yalcin, K. C. Popat, J. C. Aldridge, T. A. Desai, J. Hryniewicz, N. Chbouki, B. E. Little, O. King, V. Van, and S. Chu, IEEE J. Sel. Top. Quantum Electron. **12**(1), 148 (2006).
[18]Q. Xu, D. Fattal, and R. G. Beausoleil, Opt. Express **16**(6), 4309 (2008).
[19]S. Nakaharai, T. Tezuka, N. Sugiyama, Y. Moriyama, and S.-I. Takagi, Appl. Phys. Lett. **83**(17), 3516 (2003).
[20]Y. Liu, M. D. Deal, and J. D. Plummer, Appl. Phys. Lett. **84**(14), 2563 (2004).
[21]K. H. Lee, S. Bao, L. Zhang, D. Kohen, E. Fitzgerald, and C. S. Tan, Appl. Phys. Express **9**(8), 086501 (2016).
[22]K. H. Lee, Y. H. Tan, A. Jandl, E. A. Fitzgerald, and C. S. Tan, J. Electron. Mater. **42**(6), 1133 (2013).
[23]Y. H. Tan and C. S. Tan, Thin Solid Films **520**(7), 2711 (2012).
[24]S. Vincent, I. Radu, D. Landru, F. Letertre, and F. Rieutord, Appl. Phys. Lett. **94**(10), 101914 (2009).
[25]Y. Vlasov and S. McNab, Opt. Express **12**(8), 1622 (2004).
[26]G. Li, J. Yao, H. Thacker, A. Mekis, X. Zheng, I. Shubin, Y. Luo, J.-H. Lee, K. Raj, and J. E. Cunningham, Opt. Express **20**(11), 12035 (2012).